DOI: 10.26599/FSHW.2025.9250604



Contents lists available at SciOpen

Food Science and Human Wellness

journal homepage: https://www.sciopen.com/journal/2097-0765

China Food Publishing Co.

# Effect of the nanoscale S-layer protein armoring on tolerance, adhesion, and colonization potential of *Bifidobacterium adolescentis* Bf 15703

Guangfu Zhang[a], Jie Gao[a]*, Meiqi Li[a], Fangkun Zhao[a], Xinhui Wang[a], Qiying Zhou[a], Faizan Ahmed Sadiq[b]*, Yaxin Sang[a]*

[a]*Department of Food Science and Technology, Hebei Agricultural University, Baoding 071000, Hebei, China;*

[b]*Advanced Therapies Group, Cardiff School of Dentistry, Heath Park, Cardiff University, Cardiff, UK*

**ABSTRACT:** A proteinaceous surface layer (known as an S-layer) of numerous lactic acid bacteria has been shown to confer tissue adherence, specifically to epithelial cells, and protection against environmental stress. To investigate the potential of recombinant S-layer proteins to assemble on *Bifidobacterium*, we co-incubated S-layer proteins with *Bifidobacterium adolescentis* Bf 15703. This process resulted in a significant increase in fluorescence intensity at 533 nm compared to the control group, alongside a notable shift in zeta potential from −45.36 ± 4.05 mV to −24.31 ± 2.35 mV, confirming successful protein assembly. Morphological characterization of the armored bacteria supported these findings. *In vitro* digestion assays demonstrated significantly enhanced gastrointestinal tolerance in the modified bacterial cells. Furthermore, adhesion to HT-29 cells (a human colorectal adenocarcinoma cell line) was increased by approximately fivefold, with an adhesion rate of 1.05%. *In vivo* studies revealed a significantly prolonged retention time, as supported by *ex vivo* optical imaging and cryosection analysis. qPCR analysis confirmed sustained colonization for > 27 days. These results demonstrate that heterologously expressed S-layer proteins can successfully assemble on *B. adolescentis* Bf 15703, thereby enhancing its gastrointestinal resilience, adhesion, and long-term colonization capabilities *in vivo*.

**Keywords:** S-layer proteins; armored bacteria; gut colonization; Probiotics

## 1. Introduction

Probiotics are widely recognized for a wide range of health benefits they confer to the host, including immunomodulation, neuromodulation, digestive support, and their pivotal role in maintaining and balancing the gut microbiota. Numerous studies have demonstrated that probiotics enhance the intestinal barrier by promoting the expression and function of tight junctions between intestinal epithelial cells, produce bioactive substances like short-chain fatty acids (SCFAs), and maintain intestinal microecological balance by generating antibacterial substances such as bacteriocins, which inhibit pathogenic bacterial growth [1]. Additionally, probiotics can directly interact with immune cells in the intestine, stimulating these cells to produce antibodies and cytokines, thereby enhancing the immune response [2]. With the growing body of

***Corresponding author**
Jie Gaoa, gaojiehbu@163.com,
Faizan Ahmed Sadiqb, SadiqF@cardiff.ac.uk
Yaxin Sanga, yxsang1418@163.com

Received 15 November 2024
Received in revised from 27 January 2025
Accepted 4 March 2025

evidence-based knowledge highlighting the significant role of probiotics in health, the demand for probiotics in both food products and dietary supplements has dramatically increased.

Numerous studies [3, 4] have pinpointed that survival challenges in the gastrointestinal tract, coupled with residence time and colonization capacity in the intestine, are critical factors in the effectiveness of oral probiotics. Efforts to enhance their gastrointestinal tolerance and intestinal colonization ability have evolved, starting with the use of simple protectants like dextrin and skimmed milk powder [5], progressing to microparticle encapsulation, and eventually to multilayer wall microencapsulation [6]. Today, single-cell encapsulation techniques [7] and biofilm-based probiotic delivery systems [8] are in the spotlight. While these methods enhance probiotic survival, they do not fully address the challenge of probiotics being "transient bacteria," making stable, long-term colonization difficult [9]. The robust outer shell can hinder the direct exchange of nutrients and energy between the bacteria and their environment, potentially slowing down their growth and proliferation [10]. Therefore, the ideal protective strategy is to arm probiotics with active substances that enhance their colonization ability and confer protection without compromising their growth and metabolism.

The surface (S) layers are the outermost self-assembling proteinaceous structures of the cell envelope, commonly found in lactobacilli [11]. They are synthesized within bacteria, transported, and ultimately form a two-dimensional crystalline array covering the entire bacterial surface. Conventional methods involve extracting S-layer proteins from bacterial surfaces using coupling agents, a process that is both labor-intensive and yields limited quantities. In this study, an engineered bacterial strain previously developed by our team was used. This strain was engineered to harbor an expression vector for S-layer proteins. This approach significantly reduces the cost of obtaining S-layer proteins. Additionally, these proteins possess specific recognition and adhesion capabilities to intestinal receptors, along with heterologous expression and self-assembly abilities [12]. S-layer proteins are often referred to as "nano-wall materials" due to their ability to form highly organized crystalline lattices on the bacterial surfaces. These structural and functional characteristics enable S-layer proteins to efficiently deliver small bioactive molecules, enhancing their stability and facilitating targeted release [13, 14]. These properties indicate that S-layer proteins could serve as effective encapsulating materials for probiotic protection and delivery, offering potential improvements in bacterial tolerance and colonization. The S-layer protein used in this study isoriginated from *Lactobacillus kefiri* isolated from Tibet kefir grains, which have been traditionally used to ferment kefir milk, a staple in the diet of nomadic communities. This long history of consumption supports the safety and edibility of the S-layer protein as a potential protective agent. Based on these characteristics, S-layer proteins may prove to be ideal carriers for probiotic delivery.

*Bifidobacterium adolescentis* is commonly found in the human intestine. It is one of the permissible strains for human consumption approved by the National Health Commission of the People's Republic of China and is also listed under the Qualified Presumption of Safety (QPS) by the European Food Safety Authority. It offers many important physiological functions, such as maintaining intestinal microecological

balance, alleviating obesity, immune regulation, and promoting nutrient absorption [15]. Studies have highlighted that *B. adolescentis* has poor gastrointestinal tolerance and a limited capacity to colonize the intestine [16]. Therefore, it is crucial to develop strategies that can enhance its survival and colonization in the harsh gastrointestinal environment without compromising its proliferative capacity and metabolism.

Building on previous research where S-layer proteins were used as carriers for small bioactive molecules, this study advances the concept by developing an S-layer protein-armored bacterial cell delivery strategy. The S-layer armor can be successfully assembled on the surface of *B. adolescentis* without hindering its growth. This novel delivery system confers multiple advantages: (1) enhanced resistance to harsh gastrointestinal conditions, including gastric acid, bile, and digestive enzymes; (2) improved adhesion to intestinal surfaces; (3) significantly prolonged retention of *B. adolescentis in vivo*; and (4) markedly increased colonization capacity. The specific recognition and adhesion properties of S-layer proteins, combined with their self-assembly capabilities, make this approach highly promising for targeted probiotic delivery. The straightforward preparation of these armored probiotics, coupled with their effective colonization, presents a compelling strategy for probiotic delivery in biomedical applications.

## 2. Materials and Methods

### *2.1 Preliminary Preparations*

#### *2.1.1 Bacterial strains, cells, animals, and culture conditions*

*B. adolescentis* Bf 15703 (referred to as Bf 15703) was sourced from Beina Chuanglian Biotechnology Co., Ltd. (Henan, China). The bacterial cells were activated in BBL liquid medium (Hope Bio-Technology Co., Ltd. Qingdao, China) for 48 h before use and were subsequently counted after cultivation on BBL agar medium (Hope Bio-Technology Co., Ltd. Qingdao, China) for additional 48 h. Both cultivation steps were performed under strict anaerobic conditions at 37 ℃.

The human adenocarcinoma cell line HT-29 was acquired from Seven Biotechnology Co., Ltd. (Beijing, China). These cells were cultured in high-glucose Dulbecco's Modified Eagle Medium (DMEM) containing 10% fetal bovine serum (Solarbio Science & Technology Co., Ltd. Beijing, China) at 37 ℃ in a 5% $CO_2$ atmosphere.

BALB/c mice, sourced from Beijing SPF Bio-Technology Co., Ltd. (China), were housed in an air-conditioned room maintained at 23±2 ℃ with 50±10% relative humidity. All mice were acclimatized for at least one week prior to experimentation. Experimental procedures were carried out in accordance with institutional and governmental regulations concerning the use of laboratory animals and were approved by the Animal Ethics Committee of Hebei Agricultural University**.** The ethical review approval number is No. 2023192.

#### *2.1.2 Extraction of S-Layer Proteins*

In this study, we utilized a previously engineered *Escherichia coli* strain constructed in our laboratory, harboring an expression vector for the *L. kefiri* S-layer protein (hereafter referred to as the S-layer protein).

Following induction, S-layer protein-expressing *E. coli* cells were harvested. The supernatant was collected following cell disruption and centrifugation, then dialyzed at 4 ℃ for 48 h with multiple buffer changes. Protein concentration was quantified using the BCA assay (Solarbio Science & Technology Co., Ltd. Beijing, China), yielding the final S-layer protein solution (with the final concentration adjusted to 1 mg/mL).

*2.1.3 Staining and Labeling of Bacteria and Proteins*

Following the method described by Li et al. (2024) [17] with appropriate modifications, *B. adolescentis* Bf 15703 was fluorescently labeled using 0.01 mmol/L carboxyfluorescein succinimidyl ester (CFSE,) obtained from Shanghai Yuanye Bio-Technology Co., Ltd. (China) to create CFSE-Bf 15703. Similarly, based on the protocol of Jiang et al. (2021) [18], 1 mg/mL FITC (Fluorescein Isothiocyanate) obtained from Beijing Solarbio Science & Technology Co., Ltd. (China) was used to label the S-layer protein. Excess dye was removed via dialysis to obtain FITC-S-layer protein (with the final concentration adjusted to 1 mg/mL).

*2.2 Construction and Characterization of S-Layer Protein Armored Bacteria*

*2.2.1 Fluorescence Intensity*

Following the experimental methods described by Meng et al. (2021) **[19]** and Kong et al. (2022) **[20]** with appropriate modifications, we designed three single-factor experiments to determine the selected conditions for S-layer protein armoring of *B. adolescentis* Bf 15703 (Bf 15703): (1) Bacteria in exponential growth phase were collected and the culture medium was removed by centrifugation. The cells were then resuspended in sterile physiological saline and adjusted to $1 \times 10^9$ CFU/mL to obtain Bf 15703. Co-incubation of Bf 15703 and FITC-S-layer protein (1 mg/mL) at varying volume ratios ($V_{1:1}$ to $V_{1:5}$) at 37 ℃ for 60 min, with fluorescence intensity measured to identify the selected ratio; (2) Under the selected ratio, co-incubation at different temperatures (22-42 ℃) for 60 min, followed by fluorescence intensity measurements to determine the selected temperature range (36-41 ℃); (3) With the selected ratio and temperature established, co-incubation for varying durations (20-100 min) was conducted, and fluorescence intensity along with bacterial survival was measured to determine the ideal incubation time, comparing the control group (Bf, incubated with Tris-HCl buffer) and the group harboring the S-layer (S-Bf, incubated with S-layer protein).

*2.2.2 Zeta Potential*

Following the method described by Meng et al. (2021) [19] with appropriate modifications, the control group (Bf) and the S-layer protein group (S-Bf) were incubated under the selected conditions determined in Section 2.2.1. After incubation, unbound S-layer proteins and ions in the buffer were removed by centrifugation, and the cells were resuspended in deionized water to measure the zeta potential.

*2.2.3 Confocal Laser Scanning Microscope (CLSM)*

Following the method described by Pan et al. (2022) [21] with appropriate modifications, after co-incubating CFSE-labeled *B. adolescentis* (CFSE-Bf 15703) and FITC-labeled S-layer protein (1 mg/mL) under selected conditions, unbound S-layer proteins were removed by centrifugation. The cells were then resuspended in saline to obtain FITC-S-Bf-CFSE. This suspension was applied to a microscope (Carl Zeiss,

Oberkochen, Germany) slide for observation. The excitation wavelength used was 533 nm for FITC and 271 nm for CFSE.

*2.2.4 Scanning Electron Microscopy (SEM)*

Referring to the experimental method of Chen et al. (2024) [22] with slight modifications, Bf and S-Bf were incubated under the selected conditions determined in Section 2.2.1. Unbound S-layer proteins were removed by centrifugation, and the resulting pellet was fixed with 2.5% glutaraldehyde solution for 24 h. After pretreatment, the samples were gold-coated and observed under a microscope (Hitachi High-Tech Corporation, Tokyo, Japan).

*2.2.5 Transmission Electron Microscopy (TEM)*

Following the method described by Zhu et al. (2024) [23] with appropriate modifications, Bf and S-Bf were fixed with 2.5% glutaraldehyde aqueous solution for 24 h. After pretreatment, the samples were embedded, sectioned, stained, and observed under a microscope (Hitachi High-Tech Corporation, Tokyo, Japan).

*2.3 Ex Vivo Gastrointestinal Digestion and Adhesion Capability Assessment*

*2.3.1 Morphology of Bacteria After Digestion*

Simulated gastric fluid (SGF) and simulated intestinal fluid (SIF) were freshly prepared before each experiment following Guo et al. (2024) [24], prepared immediately before use. To prepare SGF (pepsin activity of 780 U/mL), 1.3 g pepsin (30,000 U/g; Yuanye Bio-Technology Co., Ltd., Shanghai, China) and 1.5 g NaCl were completely dissolved in 50 mL sterile water. The solution was adjusted to pH 2 and sterilized through a 0.22 μm membrane filter. For SIF preparation, 0.06 g pancreatin (containing both trypsin and lipase activities at 4,000 U/g; Yuanye Bio-Technology Co., Ltd., Shanghai, China), 0.6 g porcine bile salts (Solarbio Science & Technology Co., Ltd., Beijing, China), 0.55 g $NaHCO_3$, and 1.5 g NaCl were dissolved in 50 mL sterile water. After adjusting to pH 8 and sterilizing through a 0.22 μm membrane filter, the resulting SIF contained trypsin and lipase activities of 4.8 U/mL each, with bile salt concentration of 0.012 g/mL. Then, 1 mL of both Bf and S-Bf samples were added to 9 mL of SGF and incubated with gentle shaking at 37 ℃ in a constant temperature incubator. After 2 h, Bf and S-Bf were recovered from SGF by centrifugation, and 9 mL of SIF was added for further incubation with shaking at 37 ℃. Samples were collected at 0, 2, and 4 h, centrifuged to remove digestive fluids, fixed with 2.5% glutaraldehyde aqueous solution for 24 h, and processed according to the methods in Section 2.2.4 for observation under a microscope.

*2.3.2 Viability Assessment After Digestion*

The experiment was conducted with reference to previous studies [25, 26], with appropriate modifications. Following a similar protocol to the simulated digestion tests described in Section 2.3.1, 100 μL samples from both the Bf and S-Bf groups were taken at three different time points: 0, 2, and 4 h, and added to a BBL agar medium (Hope Bio-Technology Co., Ltd., Qingdao, China). After 48 h of incubation, bacterial colonies were subjected to quantitative enumeration.

*2.3.3 Adhesion Rate Measurement*

Referring to the experimental method of Li et al. (2024) [27] with slight modifications, HT-29 cells ($2.5 \times 10^5$ cells/well) in good condition were seeded into six-well plates and incubated at 37 ℃ with 5% $CO_2$ for 24 h to form a cell monolayer. The medium was removed, and 1 mL from each group (Bf and S-Bf) was added to three wells per group, followed by 2 mL of DMEM medium (Solarbio Science & Technology Co., Ltd., Beijing, China). The plates were incubated for 4 h. After incubation, the cells were gently washed three times with PBS buffer (Solarbio Science & Technology Co., Ltd. Beijing, China) to remove any non-adherent Bf or S-Bf. Subsequently, trypsin (Seven Biotechnology Co., Ltd. Beijing, China) was used to digest the HT-29 cells along with the adhered bacteria. The cells were collected, resuspended in saline, and then plated on BBL agar medium (Hope Bio-Technology Co., Ltd. Qingdao, China) to calculate the adhesion rate of the bacterium in both samples (Bf and S-Bf).

*2.3.4 Confocal Laser Scanning Microscope (CLSM)*

The experiment was conducted with reference to previous studies [23], with appropriate modifications. HT-29 cells ($2.5 \times 10^5$ cells/well) were seeded into glass-bottom culture dishes (NEST Biotechnology Co., Ltd., Wuxi, China) to form a cell monolayer. Samples were prepared using *Bf* 15703 labeled with CFSE (CFSE-*Bf* 15703). Following the same treatment method as described in Section 2.3.3, the cells were washed three times with PBS buffer (Solarbio Science & Technology Co., Ltd. Beijing, China) and then directly fixed with tissue fixative. The cells were stained with 10 μg/mL 4', 6-diamidino-2-phenylindole (DAPI, Solarbio Science & Technology Co., Ltd. Beijing, China) staining solution for approximately 6 minutes, washed three times with PBS buffer, and observed under a microscope (Carl Zeiss, Oberkochen, Germany).

*2.4 In Vivo Colonization Capability Assessment*

*2.4.1 Ex Vivo Optical Imaging*

The experiment was conducted with reference to previous studies [28, 29], with appropriate modifications. The protocol used for animal experiments is illustrated in Figure 3A. After a one-week acclimatization period with unrestricted access to food and water, 8-week-old male BALB/c mice were randomized into two main groups: the control group and the S-layer protein group. Each main group was further divided into five time-point subgroups (1.5, 12, 24, 48, and 96 h). Mice in the S-layer protein group received an oral dose of 0.2 mL of S-Bf-CFSE, while those in the control group received an equal volume of Bf-CFSE, with each mouse administered a bacterial dose of 0.2 mL at $5 \times 10^9$ CFU/mL. Mice were euthanized via cervical dislocation at 1.5, 12, 24, 48, and 96 h post-administration. Gastrointestinal tracts were harvested at each time point, and the liver was collected at the 96-h time point for analysis using an imaging system (VILBER BIO IMAGING, Vallee de la Marne, France).

*2.4.2 Cryosectioning*

The experiment was conducted with reference to previous studies [23], with appropriate modifications. Cecum samples collected at the 96-h time point were fixed in a tissue fixative (Solarbio Science &

Technology Co., Ltd. Beijing, China) for 24 h followed by dehydration. The samples were subsequently embedded in a pre-cooled embedding medium (SAKURA Finetek Tokyo, Japan) and covered with additional embedding medium. Sections were prepared using a cryostat, stained with DAPI, and mounted with anti-fade mounting medium. Finally, the sections were scanned and imaged using a fluorescence scanner (3D-HISTECH, Budapest, Hungary).

*2.4.3 Long-term Colonization Capability Assessment*

The long-term colonization capability of the samples was assessed using modified methods based on previous studies [27]. The process of the animal experiment is illustrated in Figure 4A. Eight-week-old BALB/c mice (8 males and 8 females) were provided with free access to water and food. Following a one-week acclimation period, the mice were randomized into two groups as described in the above section: Bf and S-Bf, with 4 males and 4 females in each group. The S-layer protein group received an oral gavage of 0.2 mL S-Bf, while the control group received an equal volume of Bf, ensuring a bacterial dose of $1 \times 10^9$ CFU per mouse. Fecal samples were collected before gavage and at various time points post-gavage, then stored at -80 °C. Mouse body weight was measured and recorded during fecal sample collection.

Bf 15703 was divided into two portions: one for plate counting and the other for genomic DNA extraction using a bacterial genomic DNA extraction kit (TianGen Biotech, Beijing, China). The extracted DNA was serially diluted tenfold to generate a standard curve correlating live bacterial count with cycle threshold (Ct) values for the quantification of Bf 15703 in fecal samples. Genomic DNA from all fecal bacteria was extracted using a fecal genomic DNA extraction kit (Solarbio Science & Technology Co., Ltd. Beijing, China). The purity and concentration of the DNA were assessed using a NanoDrop™ 1000 spectrophotometer (NanoDrop Inc., Wilmington, Delaware, USA). Quantification of Bf 15703 in feces was performed using a Real-time PCR system (Applied Biosystems Inc., Foster City, California, USA) and the PerfectStart® Green qPCR SuperMix kit (TransGen Biotech Co., Ltd. Beijing, China). The final reaction volume was 20 μL, containing 10 μL of 2 × PerfectStart® Green qPCR SuperMix, 0.4 μL of each forward and reverse primer, 1 μL of DNA, 0.4 μL of Universal Passive Reference Dye (50×), and 7.8 μL of ddH2O. The primers used were BiADO-1 (5′-CTCCAGTTGGATGCATGTC-3′) and BiADO-2 (5′-CGAAGGCTTGCTCCCAGT-3′) [30]. The qPCR amplification was conducted under the following conditions: initial denaturation at 94 °C for 30 s, followed by 45 cycles of 94 °C for 5 s (denaturation), 60 °C for 15 s (annealing), and 72 °C for 10 s (extension).

*2.5 Statistical analysis*

All experiments were conducted in triplicate with data expressed as mean ± standard deviation. Statistical analyses were carried out using IBM SPSS Statistics 23 (IBM Corp., Armonk, NY, USA) and OriginPro 2021 (OriginLab Corporation, Northampton, MA, USA). One-way analysis of variance (ANOVA) followed by Duncan's multiple comparison test or independent Student's t-test was employed to evaluate differences between groups. Significant differences ($P < 0.05$) were indicated by distinct lowercase letters.

## 3. Results and Discussion

### *3.1 Synthesis and Characterization of S-Layer Protein Armored Bacteria*

To explore the assembly of S-layer proteins on the surface of *B. adolescentis* Bf 15703 and optimize the conditions for this process, FITC-labeled S-layer proteins were incubated with Bf 15703 under various conditions, as depicted in Figure 1A. The optimization results for the component ratio are shown in Figure 1A1. Fluorescence intensity increased with the proportion of S-layer proteins, indicating successful surface assembly on Bf 15703. The intensity reached a maximum value at a ratio of 1:3, suggesting that the binding sites on the Bf 15703 cell wall were fully occupied; therefore, this ratio was chosen as the selected value. Under this selected ratio, the fluorescence intensity increased with temperature, indicating enhanced assembly efficiency at higher temperatures (Figure 1A2). However, a significant increase in fluorescence at 42 ℃, likely due to the centrifugation of the mixture after incubation at this temperature, which caused all the proteins to precipitate out of the solution (Supplementary Fig. S1). These precipitated proteins remained during subsequent washing steps, leading to a marked increase in fluorescence. This is likely due to the environmental temperature reaching the denaturation point of the S-layer proteins, causing them to precipitate [31]. To clarify whether the S-layer proteins denature around 37 ℃, we further tested conditions between 36 ℃ and 42 ℃ (Figure 1A3). Fluorescence remained stable between 36 ℃ and 39 ℃ with 1 hour of incubation, with denaturation occurring only at 40 ℃ (Supplementary Fig. S1). Given that the selected growth temperature for Bf 15703 is 37 ℃, this temperature was selected for subsequent incubations.

Figure 1A4 presents the optimization results for incubation time. Under the selected ratio and temperature conditions, fluorescence intensity increased with incubation time. However, prolonged incubation can lead to protein denaturation and reduced viability of *B. adolescentis* Bf 15703, as shown in Figure 1A5. Compared to the control group (Bf), S-Bf group exhibited significantly improved ($P < 0.05$) survival, although cell viability decreased over time. This phenomenon occurred because we used a buffer solution as the co-incubation environment, which lacked the necessary nutrients for bacterial growth. To balance assembly efficiency and cell viability, 80 min were selected as the incubation time, achieving a cell viability of $89 \pm 4 \times 10^7$ CFU/mL and a fluorescence intensity of $4600.1 \pm 116.7$.

Additionally, S-layer proteins, which contain regions rich in positively charged basic amino acids, likely interact with negatively charged cell wall components (e.g., teichoic acid) through electrostatic forces [32]. Similarly, hydrophobic interactions, hydrogen bonding, and van der Waals forces may also play crucial roles in the assembly of S-layer proteins on the cell wall surface. Since the coverage of S-layer proteins can lead to changes in surface charge, the zeta potential was measured to evaluate S-layer protein coverage on the cell wall under optimized conditions (Figure 1A6). After incubation with S-layer proteins, the zeta potential of Bf 15703 significantly increased ($P < 0.05$) from $-45.36 \pm 4.05$ mV to $-24.31 \pm 2.35$ mV, indicating successful surface assembly. This finding aligns with previous studies by Meng and others [19] and Jiang and others [18], where encapsulation of positively charged liposomes with S-layer proteins similarly altered the zeta potential.

To further elucidate the surface modifications of *B. adolescentis* Bf 15703 following the assembly of S-layer proteins, comprehensive characterizations were conducted using CLSM, SEM, and TEM, as illustrated in Figures 1B-D. Across all imaging modalities, Bf 15703 displayed the characteristic irregular rod-shaped or V-shaped structures typical of *B. adolescentis*, as previously documented [15, 33]. In Figure 1B, CLSM was employed to visualize the bacteria, which were fluorescently labeled using carboxyfluorescein succinimidyl ester (CFSE), a dye known for its robust fluorescence stability and high detection sensitivity. CFSE binds covalently to intracellular proteins via the reaction of its succinimidyl ester group with lysine residues, producing a stable fluorescent signal that persists through cell division [34, 35]. It is noteworthy that CFSE has been proven to be non-toxic to cells and has been used in fluorescent labeling and tracking of various bacteria [36, 37]. Following S-layer protein assembly, one or more discontinuous protein patches were observed on the surface of Bf 15703. SEM imaging (Figure 1C) revealed that these patches were composed of numerous small, discontinuous protein spots, resembling an armor-like structure on the bacterial surface. Consequently, Bf 15703 incubated with S-layer proteins is referred to as "armored bacteria" (S-Bf), whereas those without S-layer protein incubation are termed "non-armored bacteria" (Bf). TEM analysis, augmented by ultrathin sectioning, provided further magnification and revealed that the S-layer protein formed a discontinuous coating with a thickness of approximately 200 nm. Notably, this armor-like coating was predominantly localized at the poles and midsection of the bacteria, correlating with regions of binary fission, suggesting a strategic assembly of S-layer proteins in relation to the bacterial cell division process. This is because the bacterial cell wall is a rather complex topological structure [38]. During bacterial proliferation, a series of enzymatic reactions orchestrate the synthesis of new peptidoglycan. Concurrently, autolysins and other specific enzymes selectively degrade portions of the existing peptidoglycan structure, facilitating the insertion of new peptidoglycan and allowing for the expansion of the cell wall. Following this, transpeptidases catalyze the formation of cross-links between newly synthesized peptidoglycan units, thereby enhancing the stability and integrity of the cell wall. As cell division approaches, peptidoglycan and other essential cellular components accumulate at the site of division, where a cell plate begins to form. This plate expands gradually, ultimately resulting in the separation of the cell into two distinct daughter cells [39, 40]. This series of enzymatic reactions leads to a rapid expansion of the cell wall area, causing the extracellular material layer covering the original cell wall at the two poles and middle region to rupture, as it cannot accommodate the increased surface area. This rupture exposes additional binding sites on the cell wall, which the S-layer proteins preferentially bind to, targeting these newly accessible regions [32]. Furthermore, after forming protein patches on the bacterial cell wall surface, S-layer proteins create molecular defects and boundaries, leading to significant changes in Gaussian curvature [41, 42]. This makes S-layer protein monomers more likely to cluster around already formed patches, forming larger patches. This also explains the varying thickness and size of protein patches observed in SEM.

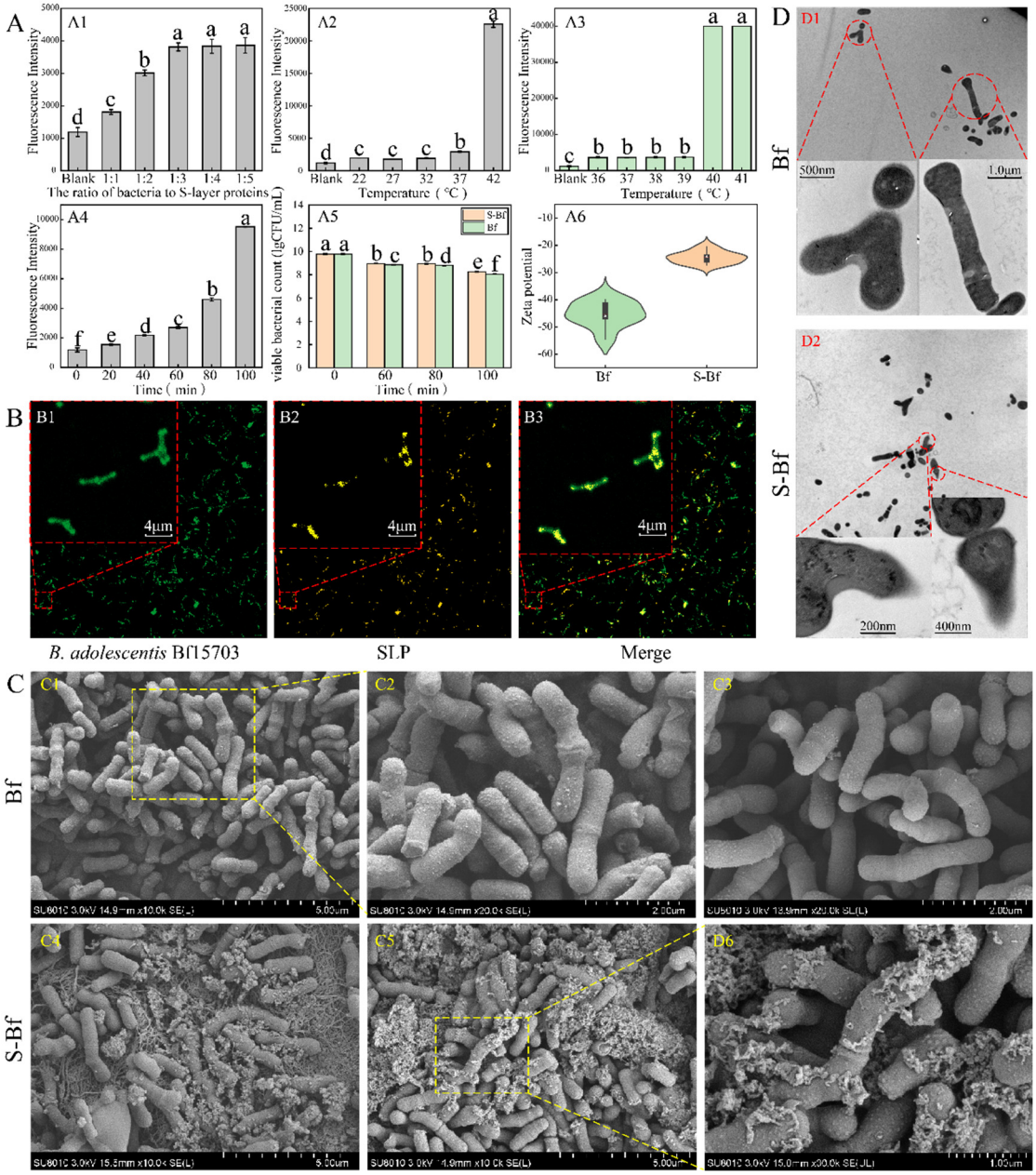


**Figure 1.** Construction and characterization results of armored bacteria. **(A)** Single-factor optimization results: Changes in fluorescence intensity after co-incubation of bacteria with varying ratios of S-layer protein **(A1)**; changes in fluorescence intensity at different temperatures during co-incubation with S-layer protein **(A2, A3)**; changes in fluorescence intensity and viable bacterial count after co-incubation with S-layer protein over different incubation times (**A4**, **A5**); changes in Zeta potential before and after co-incubation with S-layer protein **(A6)**. **(B)** Confocal laser scanning microscopy (CLSM) results after co-incubation with S-layer protein. Green indicates Bf 15703, and yellow indicates S-layer protein. **(C)** SEM results: The S-layer coated group (S-Bf) refers to co-incubation with S-layer protein, while the control group (Bf) indicates no co-incubation with S-layer protein. **(D)** TEM results. Data are presented as means ± SD (n = 3). Different letters indicate statistically significant differences ($P < 0.05$).

### *3.2 Ex Vivo Gastrointestinal Tolerance and Adhesion Capability of Armored Bacteria*

To assess the tolerance of bacterial cells that acquired the S-layer protein in the gastrointestinal tract, we conducted *in vitro* simulated digestion experiments. The SEM images for each stage of digestion are shown in Figure 2A. As digestion progressed, most non-armored bacteria (Bf) showed significant changes in their morphology such as swelling, followed by shrinking, twisting deformation, rupture, and eventually dissolution. After the simulated digestion (Figure 2A3), almost no intact bacterial cells were observed. In

contrast, the majority of armored bacteria (S-Bf) retained their normal morphology, with swelling occurring only in regions not protected by the S-layer protein. Similarly, the bacterial viability after digestion (Figure 2B) exhibited comparable trends. As digestion time increased, the viability of the bacteria decreased significantly ($P < 0.05$), but the armored bacteria (S-Bf) consistently showed higher viability than the non-armored bacteria (Bf).

Probiotics face numerous challenges in the gastrointestinal environment due to stress factors such as digestive enzymes, high acidity, bile salts, osmotic pressure changes, oxidative stress, and nutrient deprivation [43]. Hydrochloric acid and digestive enzymes can damage bacterial cell membranes and cell walls, causing bacteria to lose their structural integrity. High concentrations of bile salts can disrupt membrane permeability, leading to leakage of cellular contents, which may result in deformation or inactivation of Bf 15703. Our results indicate that the S-layer protein indeed provides effective protection for Bf 15703, likely due to its stable physicochemical properties [12], which confer resistance to changes in the external environment.

Guo et al. (2024) [24] developed microcapsules of *L. rhamnosus* GG using a co-encapsulation technique involving alginate/pectin and inulin. SEM analysis of *in vitro* digestion revealed that these microencapsulated bacteria displayed enhanced tolerance compared to non-encapsulated counterparts. However, the efficiency of intestinal release in the inulin co-encapsulated microcapsules was lower than that of the control group. This observation was interesting as the release rate of probiotics post-digestion is a key factor influencing their functional efficacy in the intestine. Unlike microencapsulation, the S-layer protein serves as a natural "protective suit" that does not hinder the exchange of substances and energy with the environment. To verify this, the effect of different concentrations of S-layer protein solution on bacterial cell growth was assessed using the CCK-8 assay (Supplementary Fig. S2). The results indicated that S-layer protein did not affect bacterial growth, which is consistent with our hypothesis. To enhance intestinal absorption of the cholesterol-lowering peptide Leu−Gln−Pro−Glu (LQPE), Jiang et al. (2021) [18] used S-layer protein-coated liposomes and control liposomes as carriers to deliver LQPE. The results showed that the S-layer protein-coated liposomes exhibited higher protective capabilities in simulated gastrointestinal fluids. Hollmann et al. (2007) [44] developed S-layer protein-coated liposomes using proteins extracted from *L. kefir* JCM 5818 and *L. brevis* JCM 1059, and assessed their stability in simulated gastrointestinal environments. Their findings demonstrated that after incubation in simulated digestive fluids for 60 and 120 min, the S-layer protein-coated liposomes retained significantly more carboxyfluorescein than uncoated control liposomes. These results suggest that S-layer proteins not only offer protective benefits during digestion but also maintain the exchange of substances between the bacterial cells and their external environment, thereby eliminating the need for a separate release mechanism.

Recent advances in probiotic delivery systems have predominantly centered on the development of wall materials with enhanced resistance properties to encapsulate probiotics, thereby bolstering their environmental tolerance. Enhancing the ability of probiotics to adhere to intestinal surfaces is crucial for successful colonization. A study by Yunyang Zhu et al. (2023) [45] demonstrated that microcapsules formed

through secondary encapsulation with mucin and gelatin or chitosan significantly improved the intestinal adhesion of probiotics. However, it is important to note that the ability of these microcapsules to release their contents within the intestine is still a critical consideration. S-layer proteins, which serve as key adhesins on the bacterial surface, play a vital role in enhancing this adhesion. To assess the intestinal adhesion ability of the S-layer protein-coated bacteria (S-Bf), *in vitro* adhesion experiments were conducted using HT-29 cells to simulate the human colon. The results, depicted in Figures 2C and 2D, indicate that S-Bf exhibited a significantly ($P < 0.05$) higher adhesion rate to HT-29 cells, approximately five times greater than that of the non-armored bacteria (Bf), achieving an adhesion rate of 1.05% (Figure 2C). Laser confocal microscopy results (Figures 2D2 and 2D5) further confirmed that S-Bf adhered more extensively to the surface of HT-29 cells. These findings suggest that S-layer proteins substantially enhance the adhesion capability of *B. adolescentis* Bf 15703, which is critical for effective colonization in the gastrointestinal environment.

Recent studies have increasingly highlighted the role of S-layer proteins in mediating bacterial adhesion to host cells, particularly gastrointestinal epithelial cells. For instance, Åvall-Jääskeläinen et al. (2003) engineered *L. lactis* NZ9000 to express the SlpA gene from *L. brevis* ATCC8287, and observed a significant increase in its adhesion to epithelial cells compared to the wild-type strain [46]. Similarly, the removal of S-layer proteins from *L. acidophilus* ATCC4356 was shown to markedly reduce its adhesion to HT-29 human colorectal cancer cells [47]. These findings suggest that S-layer proteins play a crucial role in bacterial adhesion to intestinal epithelial cells. The enhanced adhesion may be related to receptors expressed on the surface of epithelial cells and the extracellular matrix (ECM), such as fibronectin, collagen, and laminin, which bind to S-layer proteins, thereby promoting bacterial adhesion [12]. The findings from these studies, along with our experimental results, strongly support the conclusion that S-layer proteins can significantly enhance ($P < 0.05$) the intestinal adhesion ability of *B. adolescentis* Bf 15703, which is a crucial factor for effective colonization in the gastrointestinal tract.

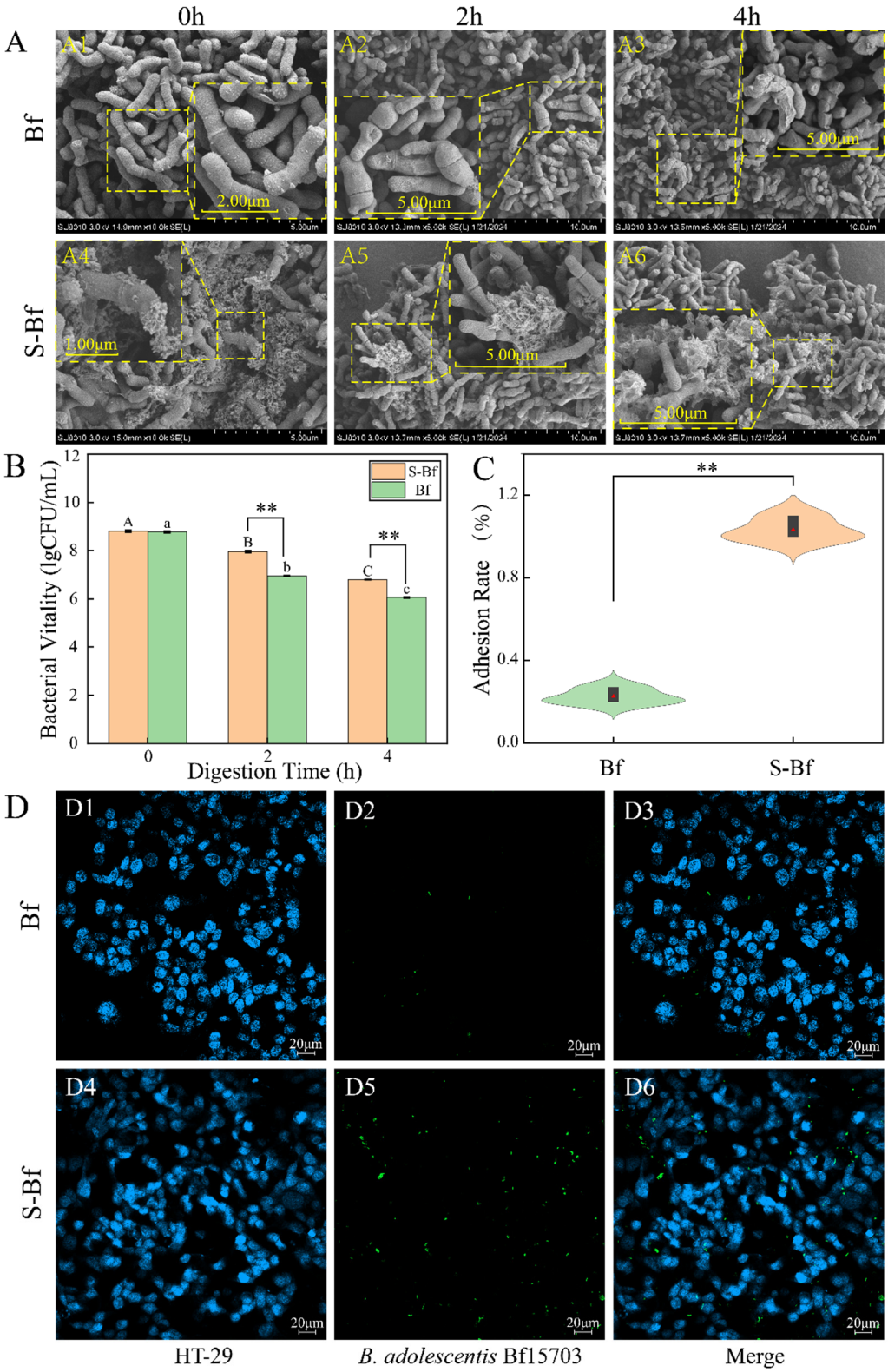


**Figure 2.** *In vitro* evaluation results of armored bacteria. **(A)** Status of armored bacteria (S-Bf) and unarmored bacteria (Bf) after *in vitro* digestion. 0 h indicates before digestion, 2 h indicates the end of the gastric digestion phase, and 4 h indicates the end of the intestinal digestion phase. **(B)** Changes in bacterial viability at different digestion stages. **(C)** Adhesion rates of armored bacteria and unarmored bacteria to HT-29 cells. **(D)** Laser confocal imaging results of armored bacteria and unarmored bacteria adhesion to HT-29 cells. Green represents Bf 15703, and blue represents the nuclei of HT-29 cells. Data are presented as means ± SD (n = 3). *$P < 0.05$), **$P < 0.01$.

### *3.3 In Vivo Adhesion and Long-term Colonization Capability of Armored Bacteria*

*In vivo* residence and behavior of the armored bacteria (S-Bf-CFSE) were evaluated using a mouse model (Figure 3A), with non-armored bacteria (Bf-CFSE) serving as the control. CFSE-labeled *B. adolescentis* Bf

15703 enabled tracking via *ex vivo* optical imaging, revealing its distribution across the digestive tract (Figure 3B). At 1.5 h post-gavage, *B. adolescentis* was detected throughout the stomach, small intestine, and cecum, likely due to rapid gastrointestinal motility induced by the influx of liquid, which stimulated gastric and intestinal peristalsis [48]. 12 h post-gavage, fluorescence persisted in the stomachs of both groups, with a more pronounced and continuous signal in the small intestine of the S-Bf group compared to the control. By 24 h, the fluorescence in the stomach had further diminished, yet the small intestine of the S-Bf group retained higher and more consistent fluorescence. At 48 h, stomach fluorescence was nearly absent in both groups; however, the S-Bf group maintained weak signals in the duodenum and jejunum and stronger signals in the ileum, with the cecum and colorectal regions showing a more intense and broader fluorescence distribution compared to the control. Finally, at 96 h, fluorescence in the stomach and small intestine had disappeared in the control group but remained detectable at the end of the ileum and in larger areas of the cecum and colon in the S-Bf group.

Additionally, fluorescence signals were detected in the liver 96 h post-gavage (Figures 3B11-12), with the control group (Bf) showing higher fluorescence intensity than the S-layer protein group (S-Bf). This observation likely results from the digestion and degradation of some bacteria as they transit through the gastrointestinal tract [49]. The CFSE-lysine covalent complexes within the bacterial cells are then released into the intestine and subsequently enter the systemic circulation via the hepatic portal vein, alongside other small molecules[50]. Consequently, a greater quantity of *B. adolescentis* from the control group (Bf) was digested and absorbed into the systemic circulation, leading to higher fluorescence intensities detected in the liver. These results align with previous studies on bacterial colonization[28, 50].

To quantify the changes in fluorescence signal intensity of armored bacteria (S-Bf) within the gastrointestinal tract, we conducted a semi-quantitative analysis using ImageJ software. Fluorescence signal intensities were measured in the stomach, small intestine, and large intestine, with the results presented in Figure 3B, followed by a significance analysis shown in Figure 3C. Over time, the fluorescence signal intensity of *B. adolescentis* Bf 15703 in both groups displayed discernible patterns. Notably, during the early digestion phase (1.5-12 h), the inherent adhesion capacity conferred by S-layer proteins caused increased retention of S-Bf samples in the stomach. Concurrently, sustained gastric acid and enzymatic digestion induced bacterial cell wall rupture, releasing CFSE covalent complexes, which led to a significant fluorescence intensity increase at 12 h. Significant differences emerged between the two groups during the mid-digestion phase (24-48 h). This may be attributed to the prolonged gastric emptying time required to process the large bacterial load, which initially masks any differences between the groups [51]. During this phase, the protective effects of the S-layer protein armor against gastric acid and digestive enzymes became evident, manifested by higher fluorescence intensity in the S-Bf group compared to the control (Bf) [12]. In the later stages, as the stomach emptied or the bacteria were fully digested, the fluorescence intensity differences between the two groups diminished, suggesting that the S-layer protein offers a degree of protection against gastric juice.

The fluorescence signal intensity changes of *B. adolescentis* Bf 15703 in the small intestine are illustrated in Figure 3C2. Both groups exhibited a decline in fluorescence signal intensity over time; however, starting from 12 h, the S-layer protein group (S-Bf) displayed significantly ($P < 0.05$) higher fluorescence signal intensity compared to the control group (Bf). Consistent with Figure 3B7, the fluorescence distribution in the small intestine was more continuous in the S-layer protein group (S-Bf) than in the control group (Bf). This continuity likely stems from the adhesive properties of the S-layer protein [12, 46], which suggests that the S-layer protein influences the transit speed of bacteria in the small intestine. Typically, prolonged retention in the small intestine would subject bacteria to increased damage. Despite this, our results indicated that bacteria in the S-layer protein group (S-Bf) not only remained longer in the small intestine but were also more effectively retained in the large intestine, highlighting the S-layer protein's exceptional protective capacity.

Figure 3C3 illustrates the changes in fluorescence signal intensity of *B. adolescentis* Bf 15703 in the large intestine. Both groups maintained relatively stable fluorescence signal intensity over time, but the intensity in the S-layer protein group (S-Bf) remained significantly ($P < 0.05$) higher than in the control group (Bf) throughout the entire observation period. This can be attributed to the bacteria's journey through the stomach and small intestine before reaching the large intestine (Figure 3D1). The surviving, adhesive strains adhere to the large intestine, where they utilize available nutrients to grow, reproduce, and synthesize essential amino acids and vitamins beneficial to the host [52]. In contrast, strains with poor viability or lacking adhesive capabilities are excreted with feces. Notably, the large intestine in mice is anatomically divided into the cecum, colon, and rectum, with the colon being shorter and containing less material. This suggests that probiotics may preferentially colonize the cecum in mice. Tissue section staining of the cecum at 96 h, followed by panoramic scanning (Figures 3D2-3), revealed that a greater number of Bf 15703 cells were retained in the cecum of the S-layer protein group (S-Bf). This finding is likely due to the S-layer protein imparting Bf 15703 with enhanced tolerance and adhesive properties, allowing it to traverse the stomach and small intestine with greater viability. These results suggest that the S-layer protein not only protects *B. adolescentis* Bf 15703 as it passes through the gastrointestinal tract but also enhances its adhesive ability, thereby prolonging the residence time of armored bacteria (S-Bf) in the large intestine and improving their retention.

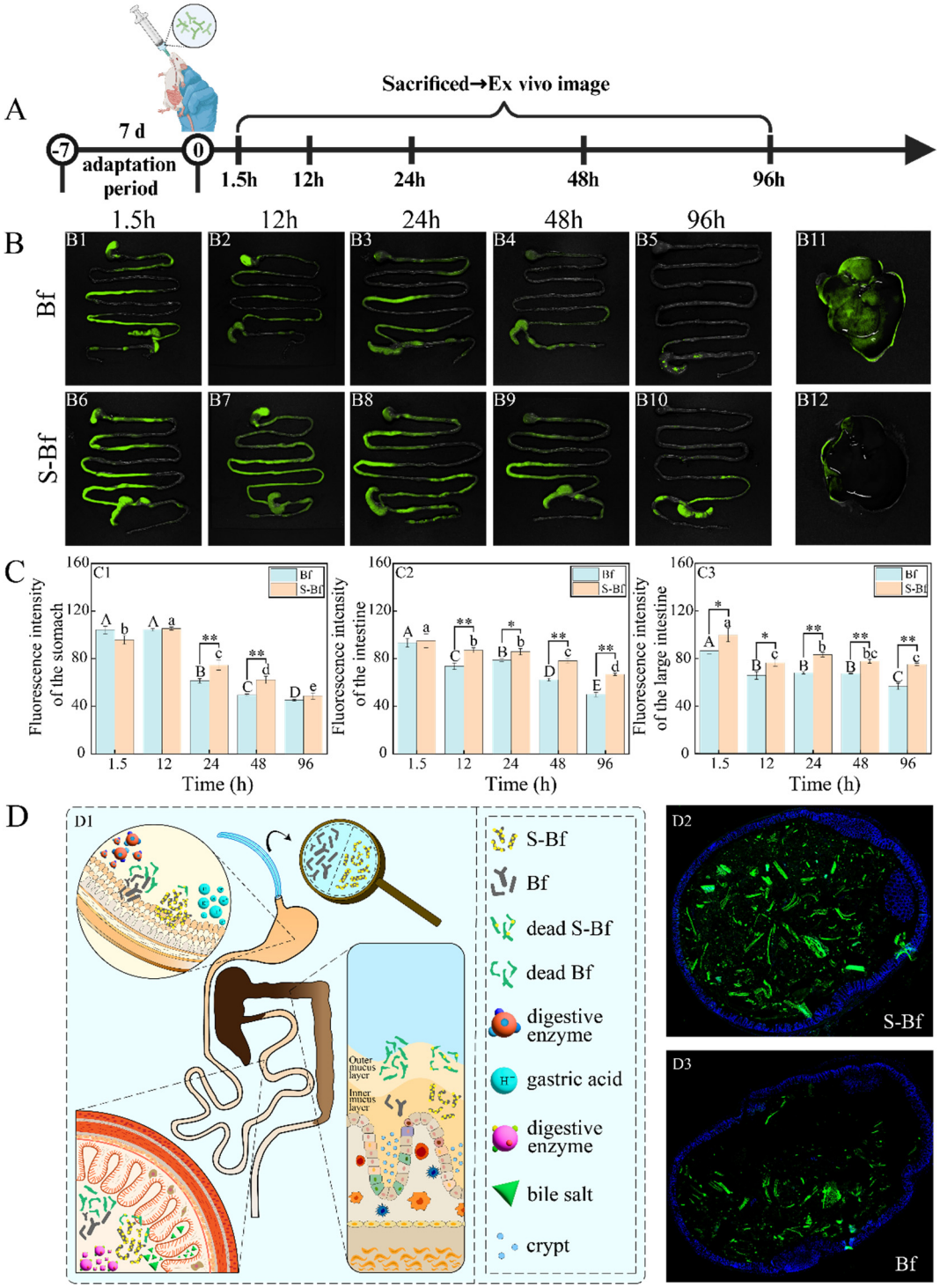


**Figure 3.** *In vivo* evaluation results of armored bacteria. **(A)** Animal experiment flowchart (Create on the BioRender platform). **(B)** *Ex vivo* optical imaging results showing the distribution of armored bacteria (S-Bf) and non-armored bacteria (Bf) in the digestive tract at different time points post-gavage. **(C)** Semi-quantitative fluorescence analysis results. Semi-quantitative analysis of fluorescence in the stomach **(C1)**, small intestine **(C2)**, and large intestine **(C3)** at different time points in B. **(D)** Diagram of bacterial distribution *in vivo*. **(D1)** Survival environment of armored and non-armored bacteria *in vivo*, **(D2)** cecum cryosection results at 96 h post-gavage with armored bacteria, and **(D3)** cecum cryosection results at 96 h post-gavage with non-armored bacteria. Data are presented as means ± SD (n = 3). Different letters indicate significant differences ($P < 0.05$). *$P < 0.05$, **$P < 0.01$.

It has been reported that *BALB/c* mice typically have either no baseline *Bifidobacteria* or, if present, only at very low levels [53]. Moreover, a review of relevant literature indicates that *BALB/c* mice are frequently used as models in studies investigating the colonization of *Bifidobacteria* [54, 55]. Our previous experiments

demonstrated that armored bacteria (S-Bf) exhibited gastrointestinal tolerance and adhesion capabilities, with significantly ($P < 0.05$) higher retention in the large intestine compared to non-armored bacteria (Bf). To further investigate whether armored bacteria can colonize the body long-term, we developed a mouse model (Figure 4A) to assess their long-term colonization ability over an extended period. We found that there was no significant change in body weight of the two groups of mice over 27 days post-gavage with either armored or non-armored bacteria (Figure 4B). At the same time, qPCR was used to quantify *B. adolescentis* Bf 15703 in mouse feces over 27 days (Figure 4C). Our results showed that the levels of Bf 15703 in the feces of both groups peaked on the fifth day and then began to decline. After 9 days, the levels of Bf 15703 in the feces of the S-layer protein group (S-Bf) stabilized after a brief fluctuation, while the control group (Bf) showed a continuous decline. Differences emerged after 13 days, with the levels of Bf 15703 in the feces of the S-layer protein group (S-Bf) being significantly ($P < 0.05$) higher than those in the control group (Bf), and this difference continued to increase in the following days. On the 27th day, the level of Bf 15703 in the feces of the S-layer protein group (S-Bf) was $7.80 \times 10^4$ CFU/g, while the level in the control group (Bf) was only $9.25 \times 10^2$ CFU/g, approximately 84 times higher in the S-layer protein group (S-Bf).

When bacteria enter the mouse digestive system, some die due to the harsh conditions within the digestive tract. Consequently, the levels of *B. adolescentis* Bf 15703 in feces initially rise and then fall within the first 9 days. Subsequently, the surviving bacteria grow and proliferate in the large intestine. Increased bacterial colonization allows for the extended detection of bacteria in feces. Li et al. (2024) [27] used qPCR to analyze rat fecal samples over a 14-days period post-gavage, concluding that galactooligosaccharides (GOS) significantly promoted the colonization of *L. plantarum* ZDY2013 in rats. The qPCR results from their study closely mirror the findings of our research. In another study Du et al. (2022) constructed a shrimp model to investigate the colonization of *L. plantarum* HC-2. The experimental group, treated with LiCl to remove surface proteins, exhibited significantly lower colonization rates compared to the control group, with prolonged LiCl treatment further decreasing bacterial numbers in shrimp intestinal segments [56]. Although a universally recognized standard for defining colonization has yet to be established, a review of colonization-related literature from the past five years (Supplementary Table S1) suggests that the detection of target bacteria in fecal samples two weeks after cessation of the intervention can be considered indicative of colonization. Our findings indicate that armored bacteria (S-Bf) possess the ability to achieve long-term colonization within the host.

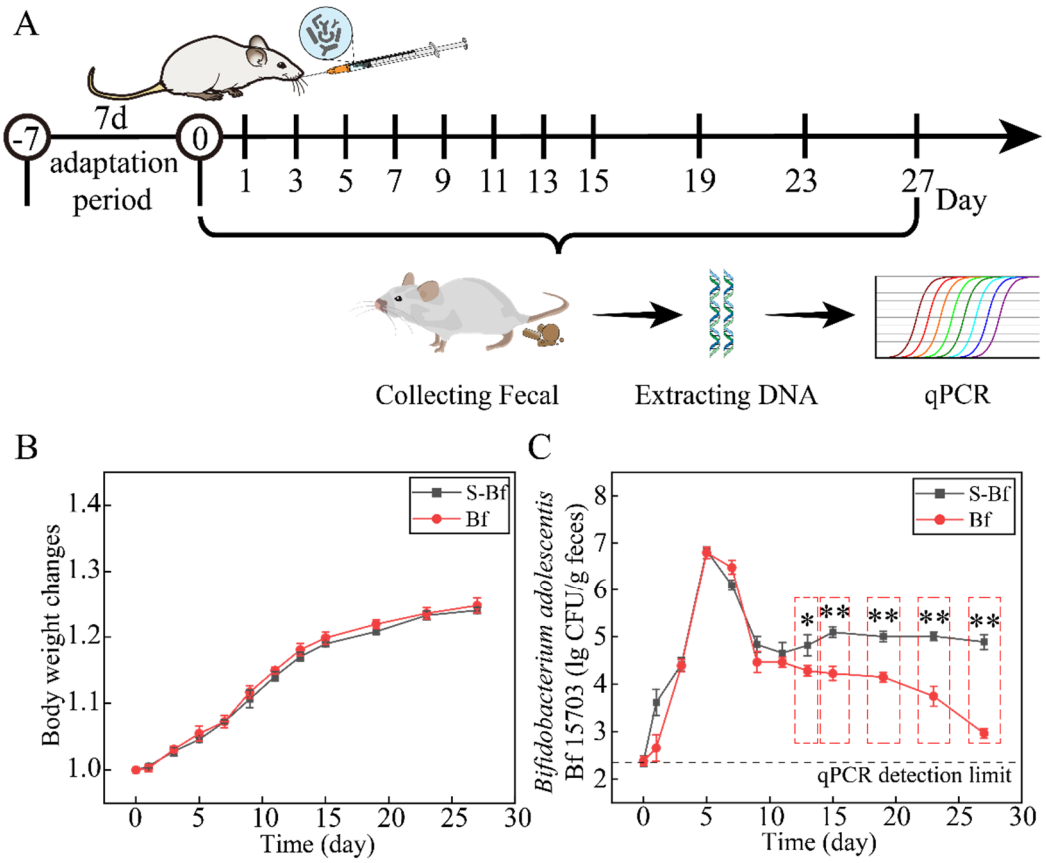


**Figure 4**. Results of long-term colonization ability of armored bacteria. **(A)** Animal experiment flowchart. **(B)** Changes in mouse body weight after gavage with armored bacteria (S-Bf) or unarmored bacteria (Bf). **(C)** Levels of Bf 15703 in mouse feces. Data are presented as means ± SD (n = 3). *$P$ < 0.05, **$P$ < 0.01.

## 4. Conclusions and Outlook

In conclusion, to address the limitations of traditional probiotic encapsulation techniques, which often fail to release their contents in a timely manner and exhibit insufficient adhesion, we developed a novel delivery strategy utilizing S-layer protein armor, which demonstrated significant advantages: enhanced protection of *B. adolescentis* Bf 15703 against gastrointestinal fluids, improved adhesion to intestinal epithelial cells, extended colonization periods, and overall enhancement of probiotic functionality. The promising results of this study suggest that S-layer protein armor could be a superior alternative to existing encapsulation methods. However, this strategy has potential limitations, such as the unknown stability of recombinant S-layer proteins during industrial production, which may present new challenges. Additionally, various environmental factors within the gastrointestinal tract, such as varying pH levels or the presence of other microbial communities, might influence the effectiveness of S-layer protein-coated probiotics, necessitating further investigation. Moreover, applying this method to other probiotic strains or used in combination with other delivery methods represents a future research direction.

## Declaration of Competing Interest

The authors declare that they have no known competing financial interests or personal relationships that could have appeared to influence the work reported in this paper.

## Data availability

No data was used for the research described in the article.

## Acknowledgements

We would like to thank BioRender for providing the platform used to create the figures in this study.

## Funding

This work was supported by the National Natural Science Foundation of China under Grant (32101911).

## References

[1] W. Fong, Q. Li, J. Yu, Gut microbiota modulation: a novel strategy for prevention and treatment of colorectal cancer, Oncogene 39(26) (2020) 4925-4943. https://doi.org/10.1038/s41388-020-1341-1.

[2] N. Guo, L.L. Lv, Mechanistic insights into the role of probiotics in modulating immune cells in ulcerative colitis, Immun. Inflamm. Dis. 11(10) (2023) e1045. https://doi.org/10.1002/iid3.1045.

[3] S. Han, Y. Lu, J. Xie, et al., Probiotic gastrointestinal transit and colonization after oral administration: a long journey, Front. Cell. Infect. Microbiol. 11 (2021) 609722. https://doi.org/10.3389/fcimb.2021.609722.

[4] I. González-Rodríguez, L. Ruiz, M. Gueimonde, et al., Factors involved in the colonization and survival of bifidobacteria in the gastrointestinal tract, FEMS Microbiol. Lett. 340(1) (2013) 1-10. https://doi.org/10.1111/1574-6968.12056.

[5] I.J. Joye, D.J. McClements, Biopolymer-based delivery systems: challenges and opportunities, Curr. Top. Med. Chem. 16(9) (2016) 1026-1039. https://doi.org/10.2174/1568026615666150825143130.

[6] H. Liu, S.W. Cui, M. Chen, et al., F. Zhong, Protective approaches and mechanisms of microencapsulation to the survival of probiotic bacteria during processing, storage and gastrointestinal digestion: a review, Crit. Rev. Food Sci. Nutr. 59(17) (2019) 2863-2878. https://doi.org/10.1080/10408398.2017.1377684.

[7] J. Han, D.J. McClements, X. Liu, et al., Oral delivery of probiotics using single-cell encapsulation, Compreh. Rev. Food Sci. Food Safety 23(3) (2024) e13322. https://doi.org/10.1111/1541-4337.13322.

[8] J. Gao, F.A. Sadiq, Y. Zheng, et al., Biofilm-based delivery approaches and specific enrichment strategies of probiotics in the human gut, Gut Microbes 14(1) (2022) 2126274. https://doi.org/10.1080/19490976.2022.2126274.

[9] Y. Xiao, Q. Zhai, H. Zhang, et al., Gut colonization mechanisms of *Lactobacillus* and *Bifidobacterium*: an argument for personalized designs, Annu. Rev. Food Sci. Technol. 12(1) (2021) 213-233. https://doi.org/10.1146/annurev-food-061120-014739

[10] C. Zhang, Z. Yu, J. Zhao, et al., Colonization and probiotic function of *Bifidobacterium longum*, J. Funct. Foods 53 (2019) 157-165. https://doi.org/10.1016/j.jff.2018.12.022.

[11] T. Sagmeister, N. Gubensäk, C. Buhlheller, et al., The molecular architecture of *Lactobacillus* S-layer: assembly and attachment to teichoic acids, Proc. Natl. Acad. Sci. 121(24) (2024) e2401686121. https://doi.org/10.1073/pnas.2401686121.

[12] G. Luo, Q. Yang, B. Yao, et al., Slp-coated liposomes for drug delivery and biomedical applications: potential and challenges, Int. J. Nanomed. 14 (2019) 1359-1383. https://doi.org/10.2147/IJN.S189935.

[13] M. Fu, S. Mi, J. Zhao, et al., The interaction mechanism, conformational changes and computational simulation of the interaction between surface layer protein and mannan at different pH levels, Food Chem 405 (2023) 135021. https://doi.org/10.1016/j.foodchem.2022.135021

[14] M. Fu, J. Gao, K. Mao, et al., Interaction mechanism between surface layer protein and yeast mannan: Insights from multi-spectroscopic and molecular dynamics simulation analyses, Food Chem 433 (2024) 137352. https://doi.org/10.1016/j.foodchem.2023.137352.

[15] C. B. Wong, T. Odamaki, J. Z. Xiao, Insights into the reason of Human-Residential Bifidobacteria (HRB) being the natural inhabitants of the human gut and their potential health-promoting benefits, FEMS Microbiol Rev 44(3) (2020) 369-385. https://doi.org/10.1093/femsre/fuaa010.

[16] T. Leser, A. Baker, *Bifidobacterium adolescentis* - a beneficial microbe, Benef Microbes 14(6) (2023) 525-551. https://doi.org/10.1163/18762891-20230030.

[17] Y. Li, Y. Pei, Z. Shan, et al., A pH-sensitive W/O/W emulsion-bound carboxymethyl chitosan-alginate hydrogel bead system through the Maillard reaction for probiotics intestine-targeted delivery, Food Hydrocolloids 153 (2024) 109956. https://doi.org/10.1016/j.foodhyd.2024.109956.

[18] X. Jiang, D. Pan, M. Tao, et al., New nanocarrier system for liposomes coated with *Lactobacillus acidophilus* S-Layer protein to improve Leu-Gln-Pro-Glu absorption through the intestinal epithelium, J Agric Food Chem 69(27) (2021) 7593-7602. https://doi.org/10.1021/acs.jafc.1c01498.

[19] J. Meng, Y. Wang, P. Hao, et al., Coating function and stabilizing effects of surface layer protein from *Lactobacillus acidophilus* ATCC 4356 on liposomes, Int J Biol Macromol 183 (2021) 457-462. https://doi.org/10.1016/j.ijbiomac.2021.04.135.

[20] W. Kong, J. Gan, M. Su, et al., Identification and characterization of domains responsible for cell wall binding, self-assembly, and adhesion of S-layer protein from *Lactobacillus acidophilus* CICC 6074, J Agric Food Chem 70(40) (2022) 12982-12989. https://doi.org/10.1021/acs.jafc.2c03907.

[21] J. Pan, G. Gong, Q. Wang, et al., A single-cell nanocoating of probiotics for enhanced amelioration of antibiotic-associated diarrhea, Nat Commun 13(1) (2022) 2117. https://doi.org/10.1038/s41467-022-29672-z.

[22] P. Chen, J. Tian, Y. Ren, et al., Enhance the resistance of probiotics by microencapsulation and biofilm construction based on rhamnogalacturonan I rich pectin, Int J Biol Macromol 258(Pt 2) (2024) 128777. https://doi.org/10.1016/j.ijbiomac.2023.128777.

[23] L. Zhu, T. Yu, W. Wang, et al., Responsively degradable nanoarmor-assisted super resistance and stable colonization of probiotics for enhanced inflammation-targeted delivery, Adv Mater 36(18) (2024) e2308728. https://doi.org/10.1002/adma.202308728.

[24] Y. Guo, Y. Liu, Q. Han, et al., Thermo-kinetic studies of *in vitro* digestion and colonic fermentation of inulin/*Lactobacillus rhamnosus* GG co-encapsulated composite beads, Food Hydrocolloids 149 (2024) 109541. https://doi.org/10.1016/j.foodhyd.2023.109541.

[25] P. Pandey, S. Mettu, H. N. Mishra, et al., Multilayer co-encapsulation of probiotics and γ-amino butyric acid (GABA) using ultrasound for functional food applications, Lwt 146(2021). https://doi.org/10.1016/j.lwt.2021.111432.

[26] X. Wang, H. Sun, J. Wu, et al., Improved viability of trehalose on *Lactobacillus plantarum* embedded with whey protein concentrate/pullulan in simulated gastrointestinal conditions and its application in acid juice, Food Science and Human Wellness 13(6) (2024) 3614-3623. https://doi.org/10.26599/FSHW.2023.9250043.

[27] J. Li, K. Shao, N. Zhang, et al., Microbiota-accessible carbohydrates enhance the biological properties and promote colonization of *Lactiplantibacillus plantarum* ZDY2013 in the intestinal tract of weaned rats, Food Bioscience 57 (2024) 103499. https://doi.org/10.1016/j.fbio.2023.103499.

[28] W. Xu, P. Su, L. Zheng, et al., *In vivo* imaging of a novel strain of Bacteroides fragilis via metabolic labeling, Front Microbiol 9 (2018) 2298. https://doi.org/10.3389/fmicb.2018.02298.

[29] Y. Wang, C. Zhang, J. Lai, et al., Noninvasive PET tracking of post-transplant gut microbiota in living mice, Eur J Nucl Med Mol Imaging 47(4) (2020) 991-1002. https://doi.org/10.1007/s00259-019-04639-3.

[30] N. V. Varankovich, N. H. Khan, M. T. Nickerson, et al., Evaluation of pea protein–polysaccharide matrices for encapsulation of acid-sensitive bacteria, Food Res. Int 70 (2015) 118-124. https://doi.org/10.1016/j.foodres.2015.01.028.

[31] H. B. Wijayanti, A. Brodkorb, S. A. Hogan, et al., Thermal denaturation, aggregation, and methods of prevention, Whey Proteins (2019) 185-247. https://doi.org/10.1016/B978-0-12-812124-5.00006-0

[32] M. M. Palomino, M. C. Allievi, T. B. Gordillo, et al., Surface layer proteins in species of the family Lactobacillaceae, Microb Biotechnol 16(6) (2023) 1232-1249. https://doi.org/10.1111/1751-7915.14230.

[33] L. He, Y. Xiong, G. Hu, et al., *Bifidobacterium spp*. as functional foods: A review of current status, challenges, and strategies, Crit Rev Food Sci Nutr 63(26) (2023) 8048-8065. https://doi.org/10.1080/10408398.2022.2054934.

[34]Y. Deng, P. Zhang, A. Wang, et al., *In vitro* study of fluorescent Dye CFSE labeled nerve cells, Life Science Instruments (2021) 22-28. https://doi.org/10.11967/2021191203.

[35] H. Tuominen-Gustafsson, M. Penttinen, J. Hytonen, et al., Use of CFSE staining of borreliae in studies on the interaction between borreliae and human neutrophils, BMC Microbiol 6 (2006) 92. https://doi.org/10.1186/1471-2180-6-92.

[36] C. Yuan, C. Zhu, Y. Bai, et al., Staining of Bartonella henselae with carboxyfluorescein diacetate succinimidyl ester for tracking infection in erythrocytes and epithelial cells, J Microbiol Methods 89(2) (2012) 102-106. https://doi.org/10.1016/j.mimet.2012.02.009.

[37] W. He, H. Liu, Z. Wang, et al., The dynamics of bacterial proliferation, viability, and extracellular polymeric substances in oral biofilm development, J Dent 143 (2024) 104882. https://doi.org/10.1016/j.jdent.2024.104882.

[38] C. J. Commerci, J. Herrmann, J. Yoon, et al., Topologically-guided continuous protein crystallization controls bacterial surface layer self-assembly, Nat Commun 10(1) (2019) 2739. https://doi.org/10.1038/s41467-019-10650-x.

[39] P. D. A. Rohs, T. G. Bernhardt, Growth and division of the peptidoglycan matrix, Annu Rev Microbiol 75 (2021) 315-336. https://doi.org/10.1146/annurev-micro-020518-120056.

[40] A. J. F. Egan, J. Errington, W. Vollmer, et al., Regulation of peptidoglycan synthesis and remodelling, Nat Rev Microbiol 18(8) (2020) 446-460. https://doi.org/10.1038/s41579-020-0366-3.

[41] N. A. Garcia, R. A. Register, D. A. Vega, et al., Crystallization dynamics on curved surfaces, Phys Rev E Stat Nonlin Soft Matter Phys 88(1) (2013) 012306. https://doi.org/10.1103/PhysRevE.88.012306.

[42] N. A. Garcia, A. D. Pezzutti, R. A. Register, et al., Defect formation and coarsening in hexagonal 2D curved crystals, Soft Matter 11(5) (2015) 898-907. https://doi.org/10.1039/c4sm02234c.

[43] V. C. D. C. Rodrigues, L. G. S. D. Silva, F. M. Simabuco, et al., Survival, metabolic status and cellular morphology of probiotics in dairy products and dietary supplement after simulated digestion, J. Funct. Foods 55 (2019) 126-134. https://doi.org/10.1016/j.jff.2019.01.046.

[44] A. Hollmann, L. Delfederico, G. Glikmann, et al., Characterization of liposomes coated with S-layer proteins from lactobacilli, Biochim. Biophys. Acta 1768(3) (2007) 393-400. https://doi.org/10.1016/j.bbamem.2006.09.009.

[45] Y. Zhu, K. Thakur, W. Zhang, et al., Double-layer mucin microencapsulation enhances the stress tolerance and oral delivery of *Lactobacillus plantarum* B2, Food Hydrocolloids 141 (2023) 108678. https://doi.org/10.1016/j.foodhyd.2023.108678.

[46] S. Avall-Jaaskelainen, A. Lindholm, A. Palva, Surface display of the receptor-binding region of the *Lactobacillus brevis* S-layer protein in *Lactococcus lactis* provides nonadhesive *lactococci* with the ability to adhere to intestinal epithelial cells, Appl. Environ. Microbiol. 69(4) (2003) 2230-2236. https://doi.org/10.1128/AEM.69.4.2230-2236.2003.

[47] Q. Yin, D. Pan, Y. Guo, et al., Effects of *Lactobacillus acidophilus* S-layer protein on adhesion to intestinal cells and macrophage proliferation, Modern Food Sci. Technol. 31 (2015) 51–55. https://doi.org/10.13982/j.mfst.1673-9078.2015.9.009.

[48] P. Padmanabhan, J. Grosse, A. B. Asad, et al., Gastrointestinal transit measurements in mice with 99mTc-DTPA-labeled activated charcoal using NanoSPECT-CT, EJNMMI Res. 3(1) (2013) 60. https://doi.org/10.1186/2191-219X-3-60.

[49] J. Shan, J. Liu, Y. Wang, et al., Digestion and residue stabilization of bacterial and fungal cells, protein, peptidoglycan, and chitin by the geophagous earthworm Metaphire guillelmi, Soil Biol. Biochem. 64 (2013) 9-17. https://doi.org/10.1016/j.soilbio.2013.03.009.

[50] W. Wang, Q. Yang, Y. Du, et al., Metabolic labeling of peptidoglycan with NIR-II Dye enables *in vivo* imaging of gut microbiota, Angew. Chem. Int. Ed. 59(7) (2020) 2628-2633. https://doi.org/10.1002/anie.201910555.

[51] F. Izbeki, T. Wittmann, S. Csati, et al., Opposite effects of acute and chronic administration of alcohol on gastric emptying and small bowel transit in rat, Alcohol Alcohol 36(4) (2001) 304-308. https://doi.org/10.1093/alcalc/36.4.304.

[52] S. R. Gill, M. Pop, R. T. Deboy, et al., Metagenomic analysis of the human distal gut microbiome, Science 312(5778) (2006) 1355-1359. https://doi.org/10.1126/science.1124234.

[53] Y. Xiao, J. Zhao, H. Zhang, et al., Mining *Lactobacillus* and *Bifidobacterium* for organisms with long-term gut colonization potential, Clin. Nutr. 39(5) (2020) 1315-1323. https://doi.org/10.1016/j.clnu.2019.05.014.

[54] M. O'Connell Motherway, A. Zomer, S. C. Leahy, et al., Functional genome analysis of *Bifidobacterium breve* UCC2003 reveals type IVb tight adherence (Tad) pili as an essential and conserved host-colonization factor, Proc. Natl. Acad. Sci. U. S. A. 108(27) (2011) 11217-11222. https://doi.org/10.1073/pnas.1105380108.

[55] F. Turroni, F. Serafini, E. Foroni, et al., Role of sortase-dependent pili of *Bifidobacterium bifidum* PRL2010 in modulating bacterium-host interactions, Proc. Natl. Acad. Sci. U. S. A. 110(27) (2013) 11151-11156. https://doi.org/10.1073/pnas.1303897110.

[56] Y. Du, H. Li, J. Shao, et al., Adhesion and colonization of the probiotic *Lactobacillus plantarum* HC-2 in the intestine of litopenaeus vannamei are associated with bacterial surface proteins, Front. Microbiol. 13 (2022) 878874. https://doi.org/10.3389/fmicb.2022.878874.